This article was downloaded by:
On: *25 January 2011*
Access details: *Access Details: Free Access*
Publisher *Taylor & Francis*
Informa Ltd Registered in England and Wales Registered Number: 1072954 Registered office: Mortimer House, 37-41 Mortimer Street, London W1T 3JH, UK

Separation Science and Technology
Publication details, including instructions for authors and subscription information:
http://www.informaworld.com/smpp/title~content=t713708471

Sodic and Acidic Crystalline Lamellar Magadiite Adsorbents for the Removal of Methylene Blue from Aqueous Solutions: Kinetic and Equilibrium Studies

Betina Royer[a]; Natali F. Cardoso[a]; Eder C. Lima[a]; Thais R. Macedo[b]; Claudio Airoldi[b]
[a] Institute of Chemistry, Federal University of Rio Grande do Sul, Porto Alegre, RS, Brazil [b] Institute of Chemistry, University of Campinas, Campinas, SP, Brazil

Online publication date: 07 January 2010

To cite this Article Royer, Betina , Cardoso, Natali F. , Lima, Eder C. , Macedo, Thais R. and Airoldi, Claudio(2010) 'Sodic and Acidic Crystalline Lamellar Magadiite Adsorbents for the Removal of Methylene Blue from Aqueous Solutions: Kinetic and Equilibrium Studies', Separation Science and Technology, 45: 1, 129 — 141
To link to this Article: DOI: 10.1080/01496390903256257
URL: http://dx.doi.org/10.1080/01496390903256257

PLEASE SCROLL DOWN FOR ARTICLE

Full terms and conditions of use: http://www.informaworld.com/terms-and-conditions-of-access.pdf

This article may be used for research, teaching and private study purposes. Any substantial or systematic reproduction, re-distribution, re-selling, loan or sub-licensing, systematic supply or distribution in any form to anyone is expressly forbidden.

The publisher does not give any warranty express or implied or make any representation that the contents will be complete or accurate or up to date. The accuracy of any instructions, formulae and drug doses should be independently verified with primary sources. The publisher shall not be liable for any loss, actions, claims, proceedings, demand or costs or damages whatsoever or howsoever caused arising directly or indirectly in connection with or arising out of the use of this material.

Separation Science and Technology, 45: 129–141, 2010
Copyright © Taylor & Francis Group, LLC
ISSN: 0149-6395 print/1520-5754 online
DOI: 10.1080/01496390903256257

Taylor & Francis
Taylor & Francis Group

Sodic and Acidic Crystalline Lamellar Magadiite Adsorbents for the Removal of Methylene Blue from Aqueous Solutions: Kinetic and Equilibrium Studies

Betina Royer,[1] Natali F. Cardoso,[1] Eder C. Lima,[1] Thais R. Macedo,[2] and Claudio Airoldi[2]

[1]*Institute of Chemistry, Federal University of Rio Grande do Sul, Porto Alegre, RS, Brazil*
[2]*Institute of Chemistry, University of Campinas, Campinas, SP, Brazil*

The present study reports the feasibility of two synthetic crystalline lamellar nano-silicates, sodic magadiite (Na-mag) and its converted acidic form (H-mag), as alternative adsorbents for the removal of the dye methylene blue (MB) from aqueous solutions. The ability of these adsorbents for removing the dye was explored through the batch adsorption procedure. Effects such as the pH and the adsorbent dosage on the adsorption capacities were explored. Four kinetic models were applied, the adsorption being best fitted to a fractionary-order kinetic model. The kinetic data were also adjusted to an intra-particle diffusion model to give two linear regions, indicating that the kinetics of adsorption follows multiple sorption rates. The equilibrium data were fitted to Langmuir, Freundlich, Sips, and Redlich-Peterson isotherm models. The maxima adsorption capacities for MB of Na-mag and H-mag were 331 and 173 mg g^{-1}, respectively.

Keywords adsorption; magadiite; methylene blue; nanomaterial; phyllosilicate

Downloaded At: 08:54 25 January 2011

INTRODUCTION

Industrial activities are responsible for generating large volumes of hazardous species in their wastewater effluents (1). Among those species, dyes represent an undesirable class of compounds that inevitably require special treatment, due to the fact that the simple presence of these compounds in water reduces light penetration, precluding photosynthesis of aqueous flora (2). In addition, other features associated with many dyes are those that affect humans, such as allergies, dermatitis, skin irritations, cancers, and mutagenicity (3–5). On the other hand, colored waters are aesthetically objectionable for drinking and other normal purposes (6). As expected, when industrial effluents contain traces of dyes, a purification operation before being released to the environment is required (2,6).

Several methods have been developed for synthetic dye removal from waters and wastewaters in order to decrease their impact on the environment. The most inexpensive and efficient procedure for such operations is related to adsorption (7–11), because the dye species are transferred from the water effluent to a solid phase, with a consequent decrease in the effluent concentration to reach as close as possible to a minimum amount (7–11). Subsequently, the adsorbent could be regenerated or kept in a dry place without direct contact with the environment (7–11).

From a series of inorganic natural (8,9) and synthetic materials (10–12), layered silicates and silicic acids have aroused enormous interest due to their exceptional adsorptions, cation-exchange properties, intercalations, and organofunctionalization abilities (12). All these properties infer the use of these materials for valuable potential applications as adsorbents, ion exchangers, catalysts, and molecular sieves.

The layered silicic acid families constituted of kenyaite, makatite, kanemite, octosilicate, and magadiite and comprise a defined class of compounds with distinct layered arrangements. All these pure crystalline layered materials are successfully synthesized in the laboratory by hydrothermal treatment, through controlled conditions of time, temperature, pressure, stoichiometry, and reagent ratio, to obtain these compounds principally in the sodic form, which is the preferred operational procedure. With the exception of octosilicate, all other polysilicates are also found naturally, for example, in highly alkaline lakes (13).

Despite the great importance of this class of layered compounds, the correct structure of magadiite still remains unknown. Some studies consider it to be built up of regular sheets of SiO_4 tetrahedra, with terminal oxygen atoms neutralized by sodium ions (14). To obtain crystalline magadiite in the acidic form, the original sodium cations must be ion-exchanged with hydrochloric acid (15).

Received 3 March 2009; accepted 15 July 2009.
Address correspondence to Eder C. Lima, Institute of Chemistry, Federal University of Rio Grande do Sul, UFRGS, Av. Bento Gonçalves 9500, Porto Alegre, RGS 91501-970, Brazil. Tel & Fax: +55 51 3308 7175. E-mail: profederlima@gmail.com or eder.lima@ufrgs.br

Similarly, to derivatize the silica surfaces (16), a large number of silanol groups are available, which hydrogen bond to a large number of organic polar basic compounds (17) to aid the adsorptive process or favor interaction as intercalation reactions take place (18).

The present investigation deals with the crystalline lamellar silicate sodic magadiite (Na-mag) and its converted acidic form (H-mag), as alternative adsorbents for removal of methylene blue (MB) from aqueous solutions, using a batch adsorption procedure. Methylene blue is an organic dye belonging to the phenothiazine family. It is mainly used for coloring bast (soft vegetable fibers such as jute, flax, and hemp), paper, leather, mordant cotton, silk, and wool (19). Due to its large application for coloring different industrial materials, there is a constant interest in removing it from aqueous solutions.

MATERIALS AND METHODS

Synthesis of Magadiite Material

Sodium magadiite (Na-mag) was synthesized using hydrothermal conditions as described previously (20). Briefly, a suspension of silica gel (Merck) and sodium hydroxide (Vetec) in an aqueous solution, with a molar ratio of SiO_2:NaOH:H_2O equal to 9:1:75, was heated at 420 K for 72 h in a sealed Teflon-lined vessel. The white product was then washed with water until the pH reached near neutral conditions, in order to remove the excess of hydroxide. The solid was centrifuged and dried at 320 K for 24 h. The acidic form (H-mag) was prepared at room temperature, over 24 h, by suspending the precursor Na-mag in 0.20 mol dm^{-3} hydrochloric acid (20).

Characterization

The X-ray diffraction patterns were obtained on a Shimadzu model XD3A diffractometer, with 2θ varying from 1.4 to 55°, using nickel filtered Cu K_α (1.54 nm) radiation. Infrared vibrational spectra were obtained on a MB-Bomem FTIR spectrometer, after pressing with KBr, accumulating 32 scans in the 4000 to 400 cm^{-1} region at a resolution of 4 cm^{-1}(21).

The NMR spectra were obtained on a Bruker AC300/P solid-state high-resolution spectrometer, using cross-polarization and magic angle spinning (CPMAS), at a frequency of 59.6 MHz with a rotational frequency of 15 kHz, acquisition time of 6 ms, and contact time of 5 ms for the ^{29}Si nucleus. Chemical shifts were referenced to tetramethylsilane.

SEM images were recorded using a Jeol model JSM-6360 LV scanning electron microscope, equipped with a field emission electron gun operated at 77 K and 5 kV. The samples were deposited under a thin layer of a vitreous support and dried with an acetone solution, sputter deposited prior to SEM analyses, and the resolution achieved was <5 nm.

The specific surface areas for the samples were determined by the BET (Brunauer, Emmett, Teller) multipoint technique using a volumetric apparatus (22) with a nitrogen probe. Pore size distribution was obtained by nitrogen adsorption–desorption isotherms, determined at the liquid nitrogen boiling point, using a volumetric apparatus connected to a turbo Edwards vacuum line system, employing a mercury capillary barometer (22). The data analyses were made by the BJH (Barret, Joyer, Halenda) method.

Thermogravimetric curves were obtained with a thermobalance from TA instruments 5100, TGA 2050 model, under a flow of dry nitrogen 30 $cm^3\,s^{-1}$ and at heating rate of 0.17 $K\,s^{-1}$.

The point of zero charge (pH_{pzc}) for both adsorbents was measured through mass titration (23) methods.

Solutions and Reagents

Deionized water was used throughout the experiments for all solution preparations.

The analytical grade cationic dye, methylene blue (MB) (C.I. 52030, basic blue 9, $C_{16}H_{18}N_3SCl$, as shown in Scheme 1) was obtained from Sigma and was used without further purification. The stock solution was prepared by dissolving accurately weighed dye in deionized water to obtain a concentration of 5000 mg dm^{-3}. Other solutions were obtained by diluting the stock dye solution to the required concentration. To adjust the pH of the solutions, 0.10 mol dm^{-3} sodium hydroxide or hydrochloric acid solutions were used. The pH of the solutions was measured using a Hanna (HI 255) pH meter.

Batchwise Procedure

The adsorption studies to evaluate the magadiite adsorbents in sodic (Na-mag) and acidic (H-mag) forms for MB dye removal from aqueous solutions were carried-out in triplicate using the batch adsorption procedure. For these experiments, fixed amounts of adsorbents varying from 20.0 to 200.0 mg were suspended in a series of 20.0 cm^3 of dye solution with concentrations that varied from 2.00 to 1000.0 mg dm^{-3} using 50 cm^3 glass flasks. These suspensions were stirred for suitable times from 5 to 360 min for kinetic experiments. The isotherms clearly demonstrated that a well-established plateau was obtained. The equilibrium studies were carried out using the optimized condition of 210 min at 298 ± 1 K. The pH of the dye solutions ranged from 2.0 to 10.0. Subsequently, in order to separate the adsorbents from the aqueous solutions, the flasks were centrifuged at 3600 rpm for 10 min, and aliquots of 1.0 to

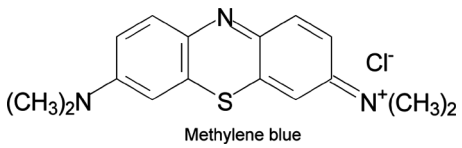

SCH. 1. Structural formula of methylene blue.

Downloaded At: 08:54 25 January 2011

$10.0\,cm^3$ of the supernatant were properly diluted. The final concentrations of the dye that remained in the solution were determined by visible spectrophotometry, using a Femto spectrophotometer provided with 1.0 cm path length optical-glass cells. Absorbance measurements were made at the maximum wavelength of MB dye of 660 nm. The MB detection limit using the spectrophotometric method, determined according to IUPAC (24), was $0.09\,mg\,dm^{-3}$.

Batch desorption studies were carried out by agitating $20.0\,cm^3$ of $200.0\,mg\,dm^{-3}$ MB solutions (pH 8.5) with 60.0 mg of Na-mag and H-mag adsorbents for 60 min. The remaining liquid phase was separated from the solid phase, and the dye loaded adsorbents, were first washed with water for removing the non-adsorbed dye. Then, the dye loaded adsorbents were agitated with 25.0 ml of aqueous solutions ($0.01–0.25\,mol\,dm^{-3}$ NaOH; $0.01–0.50\,mol\,dm^{-3}$ KCl; and $0.01–0.25\,mol\,dm^{-3}$ HCl) up to 1 h. The desorbed dye was separated and estimated as described above.

The amount of dye uptake by and the percentage of dye removal from the adsorbents were calculated by applying Eqs. (1) and (2), respectively:

$$q = [(C_o - C_f) \cdot V]/m \tag{1}$$

$$\%Removal = [100 \cdot (C_o - C_f)/(C_o)] \tag{2}$$

where q is the amount of dye uptake by the adsorbents ($mg\,g^{-1}$); C_o is the initial MB concentration in contact with the adsorbent ($mg\,dm^{-3}$), C_f is the dye concentration ($mg\,dm^{-3}$) after the batch adsorption procedure, V is the volume of dye solution (dm^3) in contact with the adsorbent, and m is the mass (g) of adsorbent.

Kinetic and Equilibrium Models

Kinetic equations corresponding to Avrami (25), pseudo first-order (26), pseudo second-order (27), Elovich (28), and the intra-particle diffusion model (29) are given in Table 1.

TABLE 1
Kinetic adsorption models

Kinetic model	Non-linear equation	Ref.
Avrami	$q_t = q_e\{1 - \exp[-(k_{AV}t)]^{nAV}\}$	(25)
Pseudo-first order	$q_t = q_e[1 - \exp(-k_f t)]$	(26)
Pseudo second order	$q_t = (k_s \cdot q_e^2 \cdot t)/(1 + q_e \cdot k_s \cdot t)$ $ho = k_s q_e^2$ initial sorption rate	(27)
Elovich	$q_t = (1/\beta)\mathrm{Ln}(\alpha\beta) + (1/\beta)\mathrm{Ln}(t)$	(28)
Intra-particle diffusion	$qt = k_{id} \cdot \sqrt{t} + C$	(29)

TABLE 2
Isotherm models

Isotherm model	Equation	Ref.
Langmuir	$q_e = (Q_{max} \cdot K_L \cdot C_e/1 + K_L \cdot C_e)$	(30)
Freundlich	$q_e = K_F \cdot C_e^{1/nF}$	(31)
Sips	$q_e = (Q_{max} \cdot K_S \cdot C_e^{1/n_s}/1 + K_S \cdot C_e^{1/n_s})$	(32)
Redlich-Peterson	$q_e = (K_{RP} \cdot C_e/1 + aRP \cdot C_e^g)$ where $0 \le g \le 1$	(33)

The isotherm equations corresponding to Langmuir (30), Freundlich (31), Sips (32), and Redlich-Peterson models (33) are listed in Table 2.

Statistical Evaluation of the Kinetic and Isotherm Parameters

The kinetic and equilibrium models were fitted by employing the nonlinear method, using the nonlinear fitting facilities of the software Microcal Origin 7.0. In addition, the models were also evaluated by an error function, which measures the differences in the amount of dye uptake by the adsorbent predicted by the models and the actual q measured experimentally (34).

$$F_{error} = \sqrt{\sum_{i}^{p} (q_{i\,model} - q_{i\,experimental}/q_{i\,experimental})^2 \cdot (1/p-1)} \tag{3}$$

where $q_{i\ model}$ is the value of q predicted by the fitted model, $q_{i\ experimental}$ is the value of q measured experimentally and p is the number of experiments performed.

RESULTS AND DISCUSSION

Adsorbent Characterization

The synthesized crystalline compounds Na-mag and H-mag (20) were characterized through X-ray diffraction (XRD) patterns, as shown in Fig. 1a. The expected lamellar structure for Na-mag is in agreement with the signals at 2θ 5.7, 11.4 and 17.1°, to give 1.55, 0.78, and 0.52 nm, which correspond to the indexed (001), (002), and (003) diffraction planes, respectively (13). Additional signals at 2θ of 23 to 30° to give the 3.83 to 2.94 nm range are also characteristic features related to the crystalline layered compound. When the precursor material is acidified to prepare H-mag, the corresponding signal due to the interlayer distance changes to 2θ 7.3° that corresponds to 1.17 nm, as shown in Fig. 1a, clearly indicating a decrease of the interlayer distance, as the sodium cation is exchanged by a proton, not only due to the difference in size, but also to the large hydration of the sodium ion (12).

Downloaded At: 08:54 25 January 2011

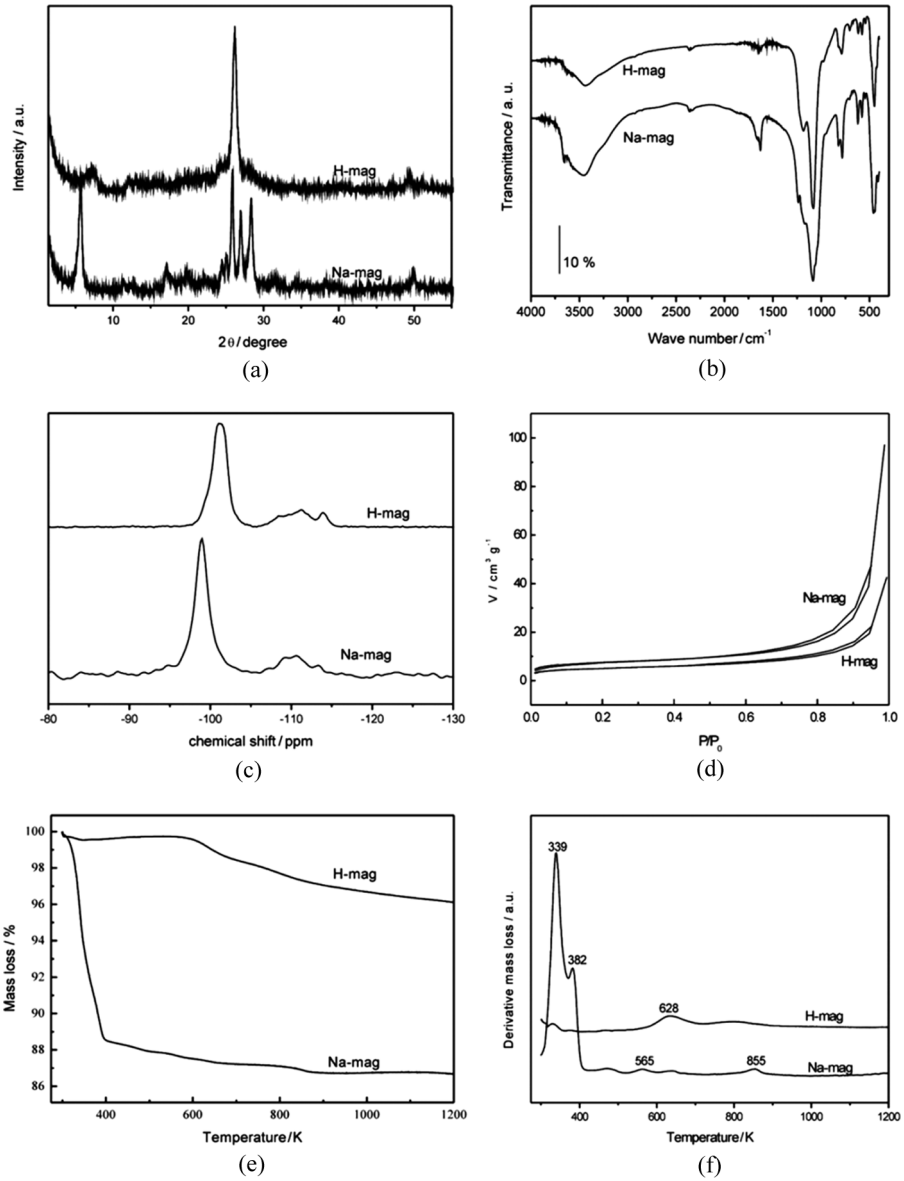

FIG. 1. A- X-ray diffraction patterns (XRD); B- IR spectroscopy; C- ^{29}Si NMR; D- N_2 adsorption/desorption isotherms; E- thermogravimetric curves, F- derivative thermogravimetric curves, for Na-mag and H-mag.

The infrared spectrum of Na-mag presents a wide band due to O−H stretching vibrations, which is attributed to the interlayer water bonded to the acidic centers on the inorganic layers and reinforced by the silanol groups in the 3640 to 3590 cm^{-1} range, followed by the out of plane vibration in the 1660 to 1628 cm^{-1} interval (15) as shown in Fig. 1b. The absorption bands of the layered silicate framework are located in the 1400 to 500 cm^{-1} region. The bands at 1000 to 1250 cm^{-1} are attributed to SiO_4 group vibrations with strong asymmetric stretching at 1075 cm^{-1}, assigned to Si-O-Si (υ_{as} Si−O−Si) and also to the terminal Si−O− (υ Si−O−) bonds. The symmetric Si−O−Si (υ_s Si−O−Si) stretching vibrations are located in the 700 to 950 cm^{-1} region and the corresponding deformation bands for Si−O−Si and O−Si−O (δ SiO) are sited in the 400 to 700 cm^{-1} interval (35). When sodium ions are exchanged by protons, the same bands for the inorganic framework are maintained, with a highly intense peak at 701 cm^{-1} in agreement with sodium replacement. Pronounced bands related to silanol groups occurred in the 3200 to 3750 cm^{-1} range (12,35), as shown in Fig. 1b.

^{29}Si NMR spectra in the solid state for sodic and acidic magadiites are shown in Fig. 1c. Through the distribution of groups containing silicon atoms on the surface it is

Downloaded At: 08:54 25 January 2011

possible to understand the characteristic structure of the inorganic layered matrices. For the sodium magadiite (Na-mag) spectrum a Q_3 signal at -99.2 ppm was observed, which is related to the $HOSi(OSi)_3$ species in the silicate sheet; however, the strongly hydrogen bonded water molecules result in a broad peak, and for the acidic form (H-mag) this signal is located at -101.1 ppm. For Q_4 signal, $Si(OSi)_4$, three peaks are observed in sodium magadiites at -109.2, -111.2, and -114.3 ppm respectively (15), while for acidic magadiite, those Q^4 signals were located at 110.9, -113.5, and -114.1 ppm. Each magadiite layer presented equal numbers of sodium cations or protons to counter the negative charge on the oxygen atoms, being as a result, neutral structures. For acidic magadiite distinguishable siloxane and silanol groups can be defined (12), which were identified by the signal displacement of the peaks.

The BET surface area results for sodic and acidic magadiites were 25.1 ± 0.1 and $16.9 \pm 0.1\ m^2\ g^{-1}$, respectively. Those crystalline layered materials present a smooth hysteresis that corresponds to the H3 type, which are associated with split-shape pores between parallel plaques. From the BJH method average pore diameters for sodic and acidic magadiites of 25 ± 1 and 19 ± 1 nm were obtained, respectively, showing a non-homogeneous pore distribution. After matrix acidification, the lamella are going to be closer together as was confirmed by X-ray diffraction patterns and, consequently, a decrease in surface area and average pore diameter for acidic magadiite is expected (20). These adsorption/desorption isotherms are shown in Fig. 1d for sodic and acidic magadiites.

The thermogravimetric and derivative curves for sodium and acidic forms for both magadiites are shown in Figs. 1e and 1f, respectively. When sodic and acidic magadiites are heated distinct masses are lost, as clearly demonstrated through the derivative curves. Thus, from the curve for Na-mag (Fig. 1e), the highest loss, shown through the derivative curve (Fig. 1f), presents two peaks at 339 and 382 K. These inflections could be interpreted as related to loss of water molecules bonded through hydrogen bonds to other similar molecules, as well as those bonded to inorganic silanol groups on the surface and finally to those bonded to the sodium ions located in the interlayer cavity, to give a total of 15.6% that corresponds to 9.2 moles of water (20). Although the general appearance of the thermogravimetric curves is similar, differences in the amount of water and in the temperatures of water release could be related to measurement conditions, when compared with other reports (15,36). Two other not well-defined mass losses were also observed for the sodium matrix at 565 and 855 K, which were attributed to inorganic framework silanol dehydroxylations to form siloxane bonds. The replacement of sodium by proton ions causes a modification of hydration capability of the sample. The thermogravimetric curves present a much lower mass loss for H-mag, as shown in Fig. 1e, which reflects in the respective derivative curve, as shown in Fig. 1f, by presenting a value of 1.6%, to give only 0.80 moles of water, as expected from the absence of Na^+ ions in the interlayer space. Very weak signals are present at 628 K, as was also previously observed (20).

The micrographs for sodic and acidic matrices are shown in Fig. 2. By comparing these images, it is possible to observe that the general morphology of the precursor Na-mag matrix is maintained even after acidic treatment to obtain H-mag. The existence of plaques (12) is clearly viewed, as expected for such layered materials.

Downloaded At: 08:54 25 January 2011

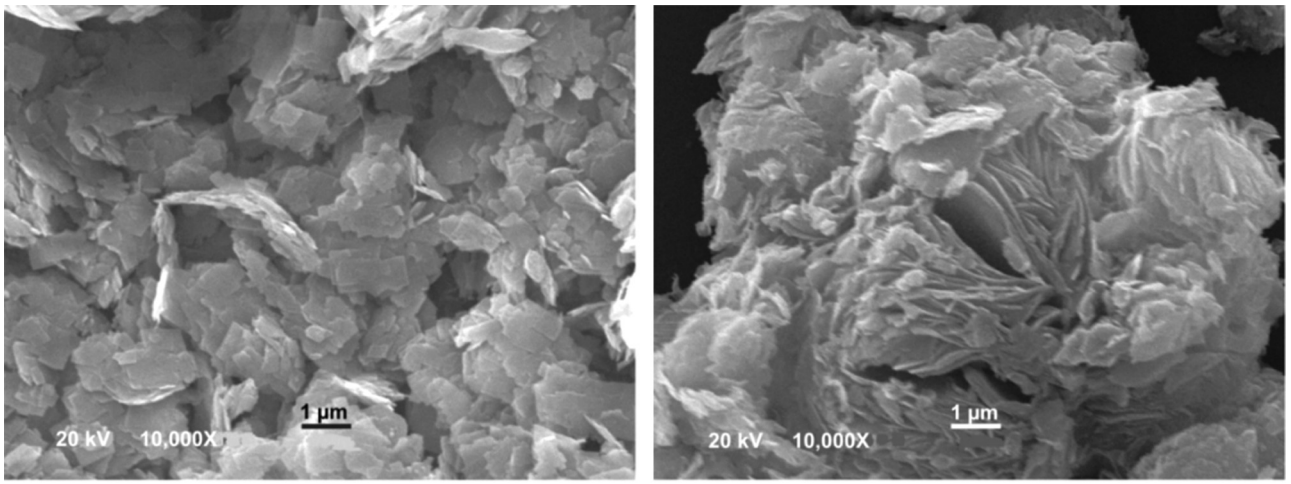

(a) (b)

FIG. 2. SEM for Na-mag (A) and H-mag (B).

Downloaded At: 08:54 25 January 2011

Effects of Acidity on Adsorption

One of the most important factors in adsorption studies is the effect of the acidity of the medium (37). Different species will present divergent ranges of suitable pH depending on which adsorbent is used. The effects of initial pH on MB dye adsorption capacity using sodic and acidic magadiite were evaluated within the pH range of 2 to 10, as shown in Fig. 3a. Dye removal increased significantly with the pH, ranging from 2.0 to 8.0 and 2.0 to 8.5 for sodic and acidic magadiites, respectively. For Na-mag, the variation of the amount of MB removal was lower than 0.3% for pH values ranging from 8.0 to 10.0. For H-mag in the pH 8.5 to 10.0 interval the variation in the percentage of removal was lower than 0.8%. Therefore, the best pH interval for MB adsorption on both sodic and acidic magadiite was from 8.5 to 10.0.

The point of zero charge (pH_{PZC}) obtained for Na-mag and H-mag were 4.5 and 3.7, respectively. For pH values higher than pH_{PZC} the adsorbent presents a negative surface charge. The higher amount of MB dye adsorbed by the two adsorbents at pH values higher than 8.5 can be explained by considering the electrostatic interactions between the surface charge of the adsorbents, which became negatively charged at pH > 4.5 and >3.7, for Na-mag and H-mag, respectively (pH > pH_{PZC}), with the positively charged MB dye. Based on these data, for both adsorbents, the pH value was fixed at 8.5.

Adsorbent Dosage

The adsorbent dosage investigation for dye removal from aqueous solution was carried out using masses of both adsorbents ranging from 20.0 to 200.0 mg, by fixing the initial concentration and volume of MB solutions at 500.0 mg dm^{-3} and 20.0 cm^3, respectively. It was observed that higher amounts of dye removal were attained for adsorbent masses of at least 60.0 mg of each adsorbent, as shown in Fig. 3b. For adsorbent masses higher than these values, the dye removal remained almost constant. The increase in the percentage of dye removal with the adsorbent mass can be attributed to the increase in the adsorbent surface areas, augmenting the number of adsorption sites available for adsorption (6,21,34). On the other hand, the increase in the adsorbent mass promotes a remarkable decrease in the amount of dye uptake per gram of adsorbent (q), as shown in Fig. 3c, an effect that

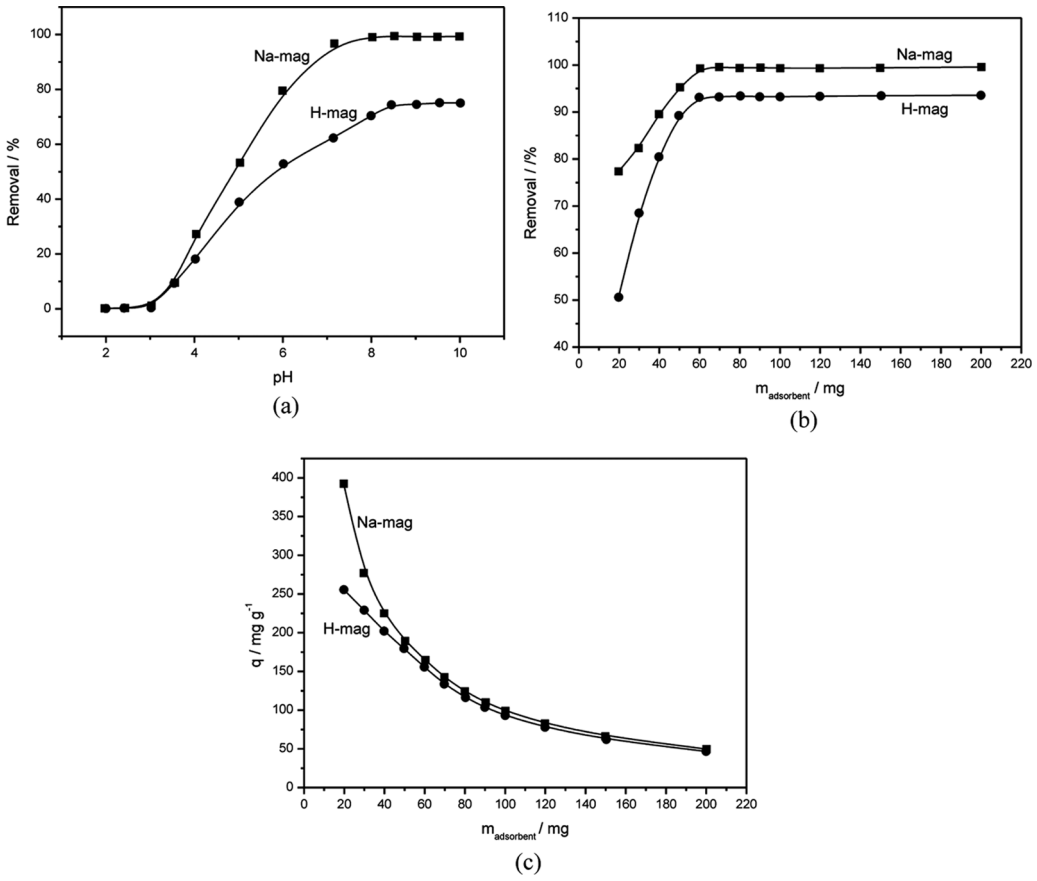

FIG. 3. Effect of pH on MB adsorption (200 mg dm^{-3}); B- Effect of adsorbent mass on the percentage of MB removal (500 mg dm^{-3}) from aqueous effluents; C- Effect of adsorbent mass on the amount of dye adsorbed. Contact time was fixed at 240 min.

can be mathematically explained by combining Eqs. (1) and (2) to give:

$$q = (\%\text{Removal} \cdot Co \cdot V)/(100 \cdot m) \quad (4)$$

As observed from Eq. (4), the amount of dye uptake (q) and the mass of adsorbent (m) are inversely proportional. For a fixed dye percentage removal, the increase of adsorbent mass leads to a decrease in q values, since the volume (V) and initial dye concentrations (C_o) are always fixed. These values clearly indicate that the adsorbent masses must be fixed at 60.0 mg for both sodic and acidic magadiites, masses that correspond to the minimum amount of adsorbent that leads to constant dye removal.

Kinetic Studies

Studies of adsorption kinetics are an important feature to be considered in aqueous effluent treatments as they provide valuable information on the mechanism of adsorption processes (21,34). In attempting to describe the dye adsorption by both adsorbents, four kinetic models were fitted, as shown in Figs. 4a and 4b. The kinetic parameters for the fitted models are listed in Table 3.

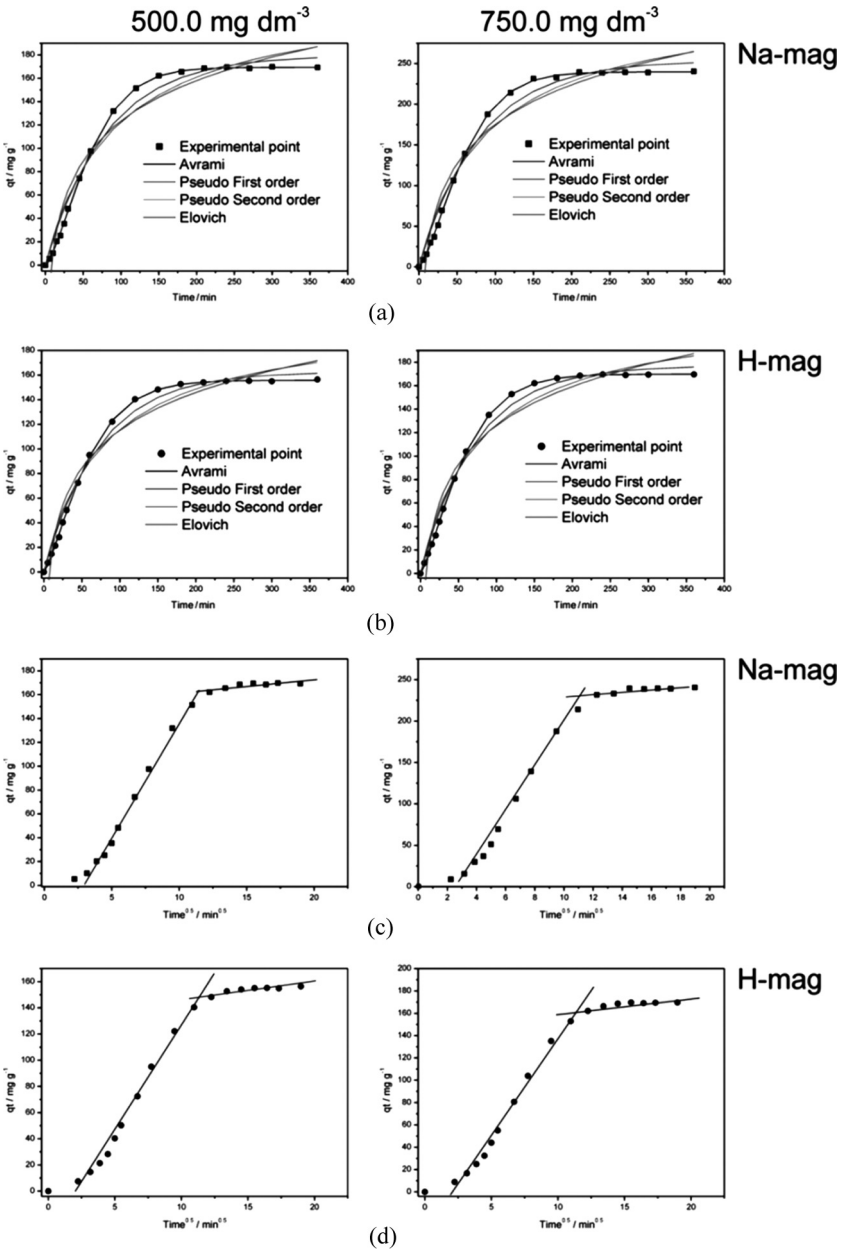

FIG. 4. Kinetic models for MB adsorption.

Downloaded At: 08:54 25 January 2011

TABLE 3
Kinetic parameters for MB removal using Na-mag and H-mag adsorbents. Conditions: temperature 298 ± 1 K at pH 8.5 and mass of adsorbent 60.0 mg

	Na-mag		H-mag	
	$500\ mg\ dm^{-3}$	$750\ mg\ dm^{-3}$	$500\ mg\ dm^{-3}$	$750\ mg\ dm^{-3}$
Avrami				
k_{AV} (min^{-1})	0.0149	0.0151	0.0157	0.0159
q_e ($mg\ g^{-1}$)	169	240	156	170
n_{AV}	1.42	1.41	1.30	1.29
R^2	0.9998	0.9997	0.9997	0.9998
F_{error}	0.0685	0.0810	0.0721	0.0780
Pseudo-first order				
k_f (min^{-1})	0.0125	0.0127	0.0137	0.0140
q_e ($mg\ g^{-1}$)	180	254	163	177
R^2	0.9852	0.9858	0.9911	0.9917
F_{error}	0.424	0.366	0.216	0.185
Pseudo-second order				
k_s ($g\ mg^{-1}\ min^{-1}$)	$5.00 \cdot 10^{-5}$	$3.00 \cdot 10^{-5}$	$6.00 \cdot 10^{-5}$	$6.00 \cdot 10^{-5}$
q_e ($mg\ g^{-1}$)	234	330	208	225
h_o ($mg\ g^{-1}\ min^{-1}$)	2.75	3.27	2.59	3.04
R^2	0.9704	0.9709	0.9770	0.9773
F_{error}	0.515	0.453	0.298	0.265
Elovich				
α ($mg\ g^{-1}\ min^{-1}$)	6.02	8.64	6.06	6.74
β ($g\ mg^{-1}$)	0.0202	0.0143	0.0227	0.0210
R^2	0.9564	0.9563	0.9618	0.9615
F_{error}	1.41	1.23	0.829	0.745
Intra-particle diffusion				
ki ($mg\ g^{-1}\ min^{-0.5}$)	19.3	25.9	16.5	18.0

*First stage.

Downloaded At: 08:54 25 January 2011

The Avrami fractionary kinetic order was suitably fitted, presenting low error function values and also high R^2 values, for the two initial concentration levels of the dye with both adsorbents. The lowest error function is followed by similar differences in calculated q values, by considering the experimentally measured model (34). It should be stressed that only the analysis of R^2 values for the establishment of a given model is not enough, because the error function evaluates the differences associated with each individual point fitted by the model, in relation to each measured experimental point. On the other hand, the R^2 value measures the differences associated with each individual point in relation to the average fitted curve (34).

Additionally, it was verified that the q_e values found in the fractionary-order were in good agreement with the experimental data. For all other models, the q values were not coincident with the q_e experimental values. These results indicate that the fractionary-order kinetic model best explains the adsorption process of MB uptake by Na-mag and H-mag adsorbents.

By analyzing the values of the kinetic parameters depicted in Table 3, it should be mentioned that the k_{AV} values showed a variation lower than 1.3%, when the initial concentration of the adsorbate increased from 500 to $750\ mg\ dm^{-3}$.

The Avrami kinetic equation has been successfully employed to explain several kinetic processes of different adsorbents and adsorbates. The Avrami exponent (n_{AV}) is a fractionary number related with the possible changes of the adsorption mechanism that take place during the adsorption process (6,21,25,28,38–43). If the mechanism of adsorption follows only an integer-kinetic order, the adsorption could follow multiple kinetic orders that are changed during the contact of the adsorbate with the adsorbent (38–43). The n_{AV} is a result of multiple kinetic orders for the adsorption procedure.

Taking into account that the kinetic results fit very well into the Avrami fractionary kinetic model for the dye using Na-mag and H-mag adsorbents, listed in Table 3 and Figs. 4a and 4b, the intra-particle diffusion model (29),

Downloaded At: 08:54 25 January 2011

was plotted in order to verify the influence of mass transfer resistance on the binding of MB to both adsorbents, as indicated by the values listed in Table 3 and shown in Figs. 4c and 4d.

The possibility of intra-particle diffusion resistance affecting adsorption was explored using the appropriate model (29). Thus, the diffusion constant, ki ($mg\,g^{-1}\,min^{-0.5}$), can be obtained from the slope of the plot of qt (uptake at any time, $mg\,g^{-1}$) versus the square root of time. Figures 4c and 4d show the plots of qt versus $t^{1/2}$, with multi-linearity for the dye using Na-mag and H-mag adsorbents. These results imply that the adsorption processes involve more than a single kinetic stage or sorption rate (43). The adsorbents exhibited two stages, which can be attributed to two linear parts, involving Figs. 4c and 4d. The first linear part can be attributed to intra-particle diffusion, which caused delay in the process. However, the second stage may be regarded as the diffusion through smaller pores, which is followed by the establishment of equilibrium (43).

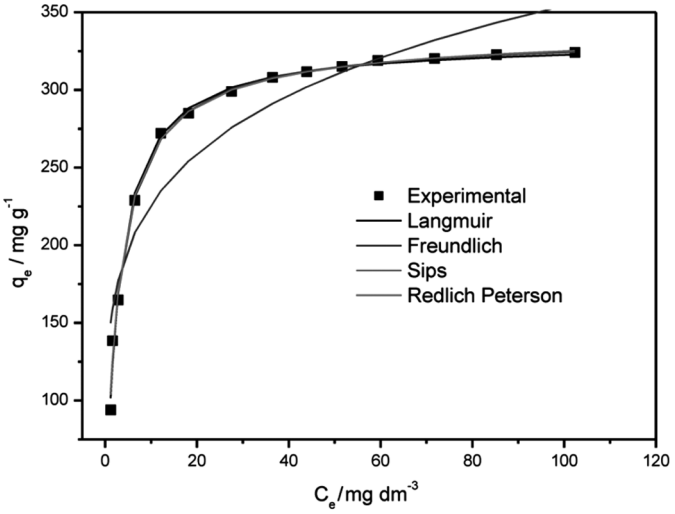

FIG. 5. Isotherm models for MB adsorption from aqueous solutions on Na-mag and H-mag adsorbents using the batch adsorption procedure at 298 ± 1 K, adsorbent mass of 60 mg; pH fixed at 8.5 for contact time of 210 min. A- Na-mag and B- H-mag.

Equilibrium Studies

The adsorption isotherm describes the amount of adsorbate uptake by the adsorbent and the adsorbate concentration that should remain in solution. Therefore, a lot of equations for analyzing experimental adsorption equilibrium data are available. The equation parameters of these equilibrium models often provide some insight into the adsorption mechanism, the surface properties and the affinity of the adsorbent. For this purpose the Langmuir (30), the Freundlich (31), the Sips (32), and the Redlich-Peterson (33) isotherm models were assayed.

The isotherms of MB adsorption on both adsorbents were performed, by using the best experimental conditions, as shown in Fig. 5, and the data of the fitted models are presented in Table 4. Based on the F_{error}, the equilibrium

TABLE 4
Isotherm parameters for MB adsorption using Na-mag and H-mag as adsorbents. Conditions: Temperature 298 ± 1 K, contact time 210 min, at pH 8.5 and mass of adsorbent 60.0 mg

	Na-mag	H-mag
Langmuir		
Q_{max} ($mg\,g^{-1}$)	331	173
K_L ($dm^3\,mg^{-1}$)	0.369	0.352
R^2	0.9952	0.9978
F_{error}	0.0401	0.0236
Freudlich		
$K_F(mg\,g^{-1}(mg\,dm^{-3})^{-1/n_F})$	145	88.7
n_F	5.14	8.01
R^2	0.8848	0.8153
F_{error}	0.185	0.194
Sips		
$Q_{max}(mg\,g^{-1})$	335	174
K_S $((mg\,dm^{-3})^{-1/n_s})$	0.381	0.379
n_S	1.06	1.08
R^2	0.9956	0.9988
F_{error}	0.0421	0.0129
Redlich-Peterson		
K_{RP} ($dm^3\,g^{-1}$)	129	62.8
a_{RP} $(mg\,dm^{-3})^{-g}$	0.410	0.373
g	0.987	0.995
R^2	0.9956	0.9980
F_{error}	0.0410	0.0203

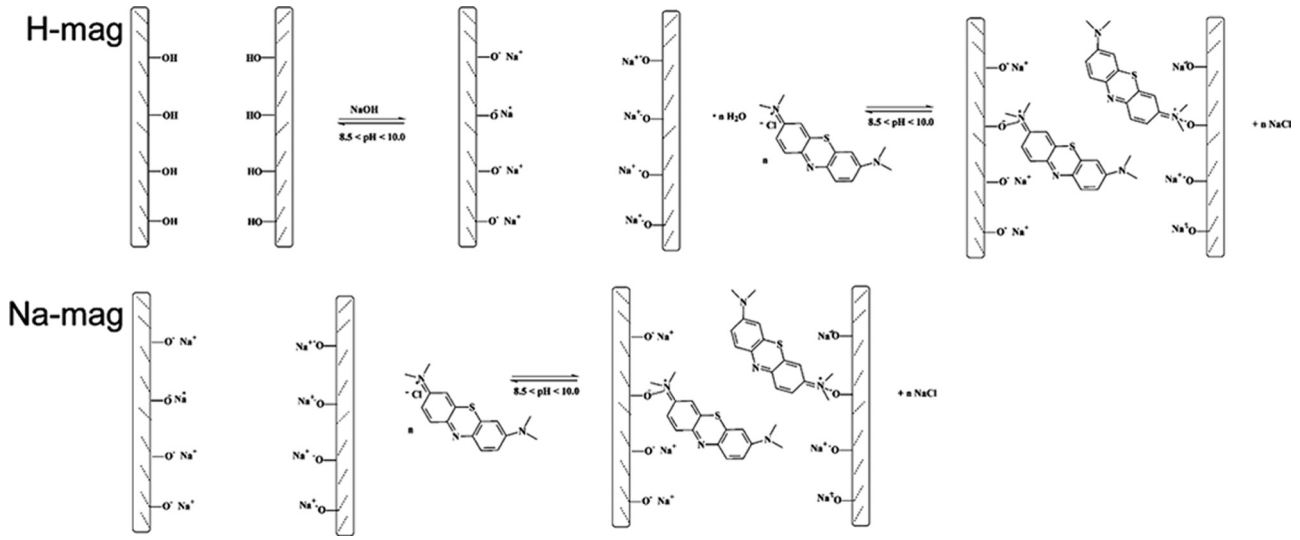

SCH. 2. Mechanism of adsorption of methylene blue on Na-mag and H-mag.

data fit very well all the isotherm models for both adsorbents, with the exception of the Freundlich model. For Na-mag, the results fit slightly better to the Langmuir isotherm model and for H-mag to the Sips isotherm model, whose results were corroborated by the R^2 value.

Taking into account that the equilibrium results were practically coincident for the Langmuir, the Sips, and the Redlich-Peterson isotherm models, the maximum amounts of MB uptake were 331 and 173 mg g^{-1} for Na-mag and H-mag, respectively. From the viewpoint of the interacting exchanger process at the solid/liquid interface, the adsorption of MB by the adsorbents should follow the mechanism depicted in Scheme 2. For H-mag the adsorption follows two steps and for Na-mag only one step is required. For H-mag, in the first step, the lamellar silicate is equilibrated with the aqueous solution ($8.5 < pH < 10.0$), where the available silanol groups loose protons, to form interchangeable sodium silicate. In the second step for both H-mag and for Na-mag the MB is intercalated inside the lamella of the silicate, with an ion-exchange process between the positively charge of dye (MB) with the sodium cation originally bound to the silicate matrix. The ion-exchange of the dye with the lamellar silicate occurs with an expansion of the basal space, as previously observed (44). Taking into account that Na-mag presents cationic sodium ions already bonded to the layered surface, the ion-exchange mechanism is facilitated by the entrance of the guest (MB), a fact that explains its higher adsorption capacity for MB.

Desorption Experiments

Desorption experiments were carried-out in order to verify the possible ion-exchange mechanism of adsorption

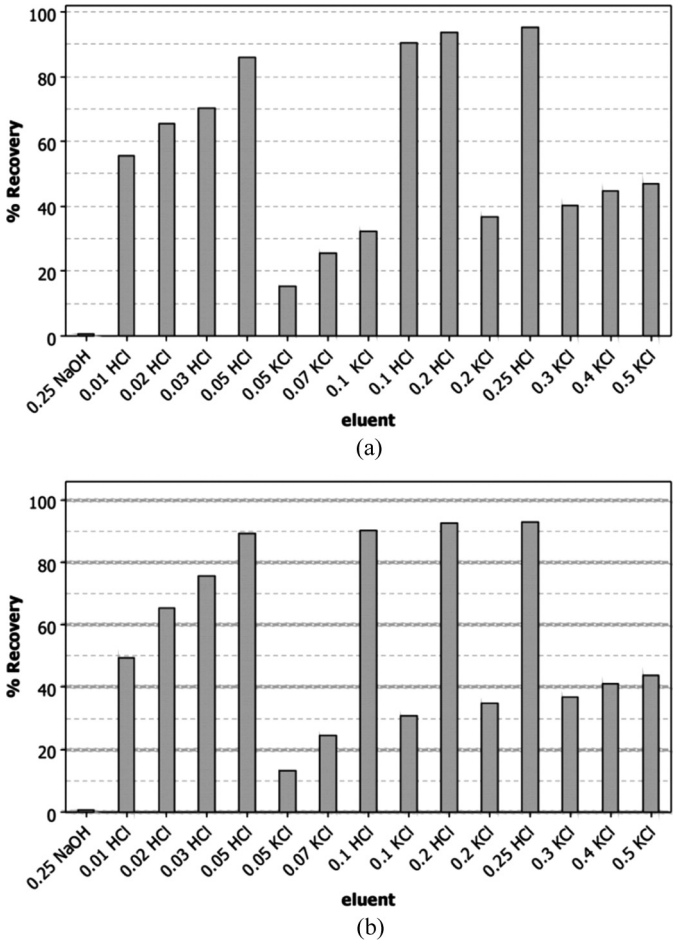

FIG. 6. Desorption of MB loaded on Na-mag (a) and on H-mag (b) adsorbents with solutions expressed by concentration in mol dm^{-3}. Desorption experiments were carried out at 298 K during 1 h.

Downloaded At: 08:54 25 January 2011

of MB on Na-mag and H-mag adsorbents, as well as to test the reusability of the adsorbents in industrial applications (see Fig. 5). It was observed that NaOH did not lead to any removal of the MB dye loaded adsorbents after 1 h of contact time (see Fig. 6). The desorption experiments carried-out with KCl promoted a fair regeneration of the MB loaded Na-mag (<47%) and MB loaded H-mag adsorbents (<44%) after 1 h of contact (see Fig. 5). The immediate desorption (<10 min) of MB from Na-mag and H-mag was achieved by using HCl solutions (see Fig. 5). These results reinforce the ion-exchange mechanism of adsorption of MB on Na-mag and H-mag adsorbents, already explained above. The recuperated adsorbents were again employed for MB dye adsorption, after regeneration of the adsorbents with 0.25 mol dm^{-3} of sodium hydroxide. No significant losses of adsorption capacity (<1.5%), were observed during the 5 cycles of adsorption/desorption using both adsorbents.

These results are important from the economic point of view, since industrial effluents contaminated with MB (19) could be treated with the Na-mag and H-mag adsorbents, using stirred tank reactors that were simulated by the batch adsorption procedure described in this work.

Downloaded At: 08:54 25 January 2011

Comparison of Different Inorganic Adsorbents for MB Adsorption

A comparison of several inorganic adsorbents employed for MB adsorption is listed in Table 5 (8,45–54). As observed, the Na-mag and H-mag adsorbents employed in this investigation present very high adsorption capacities for the dye when compared with several other inorganic adsorbents. By considering a set of eighteen adsorbents, Na-mag presented higher sorption capacity than fifteen of them (8,45–54), and H-mag showed to be more efficient than eleven of this same series of adsorbents (8,45–54). These outstanding sorption capacities place Na-mag as one of the best adsorbents and H-mag in an intermediate position in relation to the adsorption capacity for MB dye removal from aqueous solutions.

TABLE 5
Comparison of maxima adsorption capacities (MAC) of MB on different inorganic adsorbents (Ads)

Ads	MAC (mg g^{-1})	Ref.
Natural zeolite	25	8
Pyrolyzed petrified sediment	2.39	45
Activated carbon	298	46
Activated carbon	345	46
Activated carbon	385	46
Activated carbon	588	46
Acid treated diatomite	126.6	47
Palygorskite clay	51.0	48
Ordered mesoporous carbon	100.0	49
Titania-silica mesoporous materials	96	50
Activated carbo-aluminosilicate	117.9	51
Activated carbo-aluminosilicate	212.5	51
Activated carbo-aluminosilicate	325.2	51
Activated spent diatomaceous earth	56.2	52
Titania nanotubes	290	53
Natural zeolite	18.3	54
Geopolymeric adsorbents from fly ash	32.0	54
H-mag	173	This work
Na-mag	331	This work

CONCLUSION

The synthesized crystalline layered silicic sodic magadiite and its converted acidic form represent good alternative adsorbents for methylene blue removal from aqueous solutions. Both inorganic matrices have the ability to intercalate the dye inside the free cavities of the matrix at the solid/liquid interface, when the samples are suspended in water, after establishing the best conditions of pH, in the 8.5 to 10.0 range, with a minimum shaking time of 210 min, a time necessary to saturate the available centers located on the exchanger surface and to provide a well-defined isotherm. Good regenerations of the MB loaded Na-mag (95%) and H-mag (93%) adsorbents were achieved using a 0.25 mol dm^{-3} hydrochloric acid solution, reinforcing the ion-exchange mechanism. Four defined kinetic models were used to adjust the adsorption and the best fit was the Avrami (fractionary-order) model. However, the intra-particle diffusion model gave two linear regions, which suggested that the adsorption can be also followed by multiple adsorption rates. The maximum adsorption capacities were 331 and 173 mg g^{-1} for sodic and acidic magadiite, respectively. The proposed mechanism for this process can be related to the highest value obtained for the sodic form, that is caused by the facility of the dye to exchange, not only due to the ionic bonding character of this cation, but also because the process occurred in a favorable expanded basal space.

ACKNOWLEDGEMENTS

The authors are grateful to MCT, CNPq, FAPESP, and CAPES for financial support and fellowships. Prof. Carol Collins is also acknowledged for valuable language improvements.

NOTATIONS

α the initial adsorption rate (mg g^{-1} min^{-1}) of the Elovich equation.

β Elovich constant related to the extent of surface coverage and also to the activation energy involved in chemisorption (g mg^{-1}).

a_{RP} the Redlich-Peterson constant $(mg\,dm^{-3})^{-g}$.
C constant related with the thickness of boundary layer $(mg\,g^{-1})$.
C_f dye concentration at the end of the adsorption $(mg\,dm^{-3})$.
C_e dye concentration at equilibrium $(mg\,dm^{-3})$.
C_o initial dye concentration in contact with the adsorbent $(mg\,dm^{-3})$.
dq differential of q.
g dimensionless exponent of the Redlich-Peterson equation.
h_o the initial sorption rate $(mg\,g^{-1}\,min^{-1})$ of the pseudo-second order equation.
k_{AV} the Avrami kinetic constant (min^{-1}).
k_f pseudo-first order rate constant (min^{-1}).
K_F the Freundlich constant related to adsorption capacity $[mg\,g^{-1}\,(mg\,dm^{-3})^{-1/nF}]$.
k_{id} intra-particle diffusion rate constant $(mg\,g^{-1}\,min^{-0.5})$.
K_L Langmuir affinity constant $(dm^3\,mg^{-1})$.
K_{RP} Redlich-Peterson constant $(dm^3\,g^{-1})$.
K_S the Sips constant related to the affinity constant $(mg\,dm^{-3})^{-1/ns}$.
k_s the pseudo-second order rate constant $(g\,mg^{-1}\,min^{-1})$.
m mass of adsorbent (g).
n_{AV} fractionary reaction order (Avrami) which is related to the adsorption mechanism.
n_F dimensionless exponent of Freundlich equation.
n_S dimensionless exponent of Sips equation.
q amount of the dye adsorbed by the adsorbent $(mg\,g^{-1})$.
q_e amount of dye adsorbed at the equilibrium $(mg\,g^{-1})$.
Q_{max} the maximum adsorption capacity of the adsorbent $(mg\,g^{-1})$.
q_t amount of adsorbate adsorbed at time t $(mg\,g^{-1})$.
t time of contact (min).
V volume of dye in contact with the adsorbent (dm^3).

Downloaded At: 08:54 25 January 2011

REFERENCES

1. Pavan, F.A.; Gushikem, Y.; Mazzocato, A.C.; Dias, S.L.P.; Lima, E.C. (2007) Statistical design of experiments as a tool for optimizing the batch conditions to methylene blue biosorption on yellow passion fruit and mandarin peels. *Dyes Pigm.*, *72*: 256.
2. Pavan, F.A.; Lima, E.C.; Dias, S.L.P.; Mazzocato, A.C. (2008) Methylene blue biosorption from aqueous solutions by yellow passion fruit waste. *J. Hazard. Mater.*, *150*: 703.
3. de Lima, R.O.A.; Bazo, A.P.; Salvadori, D.M.F.; Rech, C.M.; Oliveira, D.P.; Umbuzeiro, G.A. (2007) Mutagenic and carcinogenic potential of a textile azo dye processing plant effluent that impacts a drinking water source. *Mutat. Res.*, *626*: 53.
4. Tsuboy, M.S.; Angeli, J.P.F.; Mantovani, M.S.; Knasmüller, S.; Umbuzeiro, G.A.; Ribeiro, L.R. (2007) Genotoxic, mutagenic and cytotoxic effects of the commercial dye CI Disperse Blue 291 in the human hepatic cell line HepG2. *Toxicol. in Vitro*, *21*: 1650.
5. Caritá, R.; Marin-Morales, M.A. (2008) Induction of chromosome aberrations in the Allium cepa test system caused by the exposure of seeds to industrial effluents contaminated with azo dyes. *Chemosphere*, *72*: 722.
6. Lima, E.C.; Royer, B.; Vaghetti, J.C.P.; Simon, N.M.; da Cunha, B.M.; Pavan, F.A.; Benvenutti, E.V.; Veses, R.C.; Airoldi, C. (2008) Application of Brazilian-pine fruit coat as a biosorbent to removal of reactive red 194 textile dye from aqueous solution. Kinetics and equilibrium study. *J. Hazard. Mater.*, *155*: 536.
7. Kavitha, D.; Namasivayam, C. (2008) Capacity of activated carbon in the removal of acid brilliant blue: Determination of equilibrium and kinetic model parameters. *Chem. Eng. J.*, *139*: 453.
8. Wang, S.; Zhub, Z.H. (2006) Characterisation and environmental application of an Australian natural zeolite for basic dye removal from aqueous solution. *J. Hazard. Mater.*, *136*: 946.
9. Gupta, V.K.; Mohan, D.; Saini, V.K. (2006) Studies on the interaction of some azo dyes (naphthol red-J and direct orange) with nontronite mineral. *J. Colloid Interface Sci.*, *298*: 79.
10. Pavan, F.A.; Dias, S.L.P.; Lima, E.C.; Benvenutti, E.V. (2008) Removal of Congo red from aqueous solution by anilinepropylsilica xerogel. *Dyes Pigm.*, *76*: 64.
11. Wang, S.; Li, H. (2006) Structure directed reversible adsorption of organic dye on mesoporous silica in aqueous solution. *Microporous Mesoporous Mater.*, *97*: 21.
12. Thiesen, P.H.; Beneke, K.; Lagaly, G. (2002) Silylation of a crystalline silicic acid: An MAS, NMR and porosity study. *J. Mater. Chem.*, *12*: 3010.
13. Fujita, I.; Kuroda, K.; Ogawa, M. (2003) Synthesis of interlamellar silylated derivatives of magadiite and the adsorption behavior for aliphatic alcohols. *Chem. Mater.*, *15*: 3134.
14. Almond, G.G.; Harris, R.K.; Franklin, K.R. (1997) A structural consideration of kanemite, octosilicate, magadiite and kenyaite. *J. Mater. Chem.*, *7*: 681.
15. Eypert-Blaison, C.; Sauzéat, E.; Pelletier, M.; Michot, L.J.; Villiéras, F.; Humbert, B. (2001) Hydration mechanisms and swelling behavior of Na-magadiite. *Chem. Mater.*, *13*: 1480.
16. Fonseca, M.G.; Silva, C.R.; Barone, J.S.; Airoldi, C. (2000) Layered hybrid nickel phyllosilicates and reactivity of the gallery space. *J. Mater. Chem.*, *10*: 789.
17. Wang, Z.; Pinnavaia, T.J. (2003) Intercalation of poly(propyleneoxide) amines (Jeffamines) in synthetic layered silicas derived from ilerite, magadiite, and kenyaite. *J. Mater. Chem.*, *13*: 2127.
18. Miyamoto, N.; Kawai, R.; Kuroda, K.; Ogawa, M. (2001) Intercalation of a cationic cyanine dye into the layer silicate magadiite. *Appl. Clay Sci.*, *19*: 39.
19. Uses of methylene blue http://www.britannica.com/EBchecked/topic/378634/methylene-blue#. Accessed on March 3rd, 2009.
20. Macedo, T.R.; Airoldi, C. (2006) Host lamellar silicic acid magadiite for some heterocyclic amine inclusions and quantitative calorimetric data. *Microporous Mesoporous Mater.*, *94*: 81.
21. Vaghetti, J.C.P.; Lima, E.C.; Royer, B.; Cardoso, N.F.; Martins, B.; Calvete, T. (2009) Pecan nutshell as biosorbent to remove toxic metals from aqueous solution. *Sep. Sci. Technol.*, *44*: 615.
22. Arenas, L.T.; Vaghetti, J.C.P.; Moro, C.C.; Lima, E.C.; Benvenutti, E.V.; Costa, T.M.H. (2004) Dabco/silica sol-gel hybrid material. The influence of the morphology on the $CdCl_2$ adsorption capacity. *Mater. Lett.*, *58*: 895.
23. Ofomaja, A.E.; Ho, Y.S. (2007) Effect of pH on cadmium biosorption by coconut copra meal. *J. Hazard. Mater.*, *139*: 356.
24. Lima, E.C.; Brasil, J.L.; Santos, A.H.D.P. (2003) Evaluation of Rh, Ir, Ru, W-Rh, W-Ir and W-Ru as permanent modifiers for the determination of lead in ashes, coals, sediments, sludges, soils, and

freshwaters by electrothermal atomic absorption spectrometry. *Anal. Chim. Acta*, *484*: 233.
25. Lopes, E.C.N.; dos Anjos, F.S.C.; Vieira, E.F.S.; Cestari, A.R. (2003) An alternative Avrami equation to evaluate kinetic parameters of the interaction of Hg(II) with thin chitosan membranes. *J. Colloid Interface Sci.*, *263*: 542.
26. Largegren, S. (1898) About the theory of so-called adsorption of soluble substances. *Kungliga Suensk Vetenskapsakademiens Handlingar*, *241*: 1.
27. Ho, Y.S.; Mckay, G.M. (1999) Pseudo-second order model for sorption process. *Proc. Biochem.*, *34*: 451.
28. Vaghetti, J.C.P.; Lima, E.C.; Royer, B.; da Cunha, B.M.; Cardoso, N.F.; Brasil, J.L.; Dias, S.L.P. (2009) Pecan nutshell as biosorbent to remove Cu(II), Mn(II) and Pb(II) from aqueous solutions. *J. Hazard. Mater.*, *162*: 270.
29. Weber-Jr., W.J.; Morris, J.C. (1963) Kinetics of adsorption on carbon from solution. *J. Sanit. Eng. Div. Am. Soc. Civil Eng.*, *89*: 31.
30. Langmuir, I. (1918) The adsorption of gases on plane surfaces of glass, mica and platinum. *J. Am. Chem. Soc.*, *40*: 1361.
31. Freundlich, H.M.F. (1906) Über die adsorption in lösungen. *Z. Phys. Chemie*, *57A*: 385.
32. Sips, R. (1948) On the structure of a catalyst surface. *J. Chem. Phys.*, *16*: 490.
33. Redlich, O.; Peterson, D.L. (1959) A useful adsorption isotherm. *J. Phys. Chem.*, *63*: 1024.
34. Vaghetti, J.C.P.; Lima, E.C.; Royer, B.; Brasil, J.L.; da Cunha, B.M.; Simon, N.M.; Cardoso, N.F.; Noreña, C.P.Z. (2008) Application of Brazilian-pine fruit coat as a biosorbent to removal of Cr(VI) from aqueous solution. Kinetics and equilibrium study. *Biochem. Eng. J.*, *42*: 67.
35. Jacques, R.A.; Bernardi, R.; Caovila, M.; Lima, E.C.; Pavan, F.A.; Vaghetti, J.C.P.; Airoldi, C. (2007) Removal of Cu(II), Fe(III) and Cr(III) from aqueous solution by aniline grafted silica gel. *Sep. Sci. Technol.*, *42*: 591.
36. Superti, G.B.; Oliveira, E.C.; Pastore, H.O.; Bordo, A.; Bisio, C.; Marchese, L. (2007) Aluminum magadiite: an acid solid layered material. *Chem. Mater.*, *19*: 4300.
37. Lima, E.C.; Royer, B.; Vaghetti, J.C.P.; Brasil, J.L.; Simon, N.M.; dos Santos-Junior, A.A.; Pavan, F.A.; Dias, S.L.P.; Benvenutti, E.V.; da Silva, E.A. (2007) Adsorption of Cu(II) on Araucaria angustifolia wastes: Determination of the optimal conditions by statistic design of experiments. *J.Hazard. Mater.*, *140*: 211.
38. Cestari, A.R.; Vieira, E.F.S.; Matos, J.D.S.; dos Anjos, D.S.C. (2005) Determination of kinetic parameters of Cu(II) interaction with chemically modified thin chitosan membranes. *J. Colloid Interface Sci.*, *285*: 288.
39. Cestari, A.R.; Vieira, E.F.S.; Pinto, A.A.; Lopes, E.C.N. (2005) Multistep adsorption of anionic dyes on silica/chitosan hybrid 1. Comparative kinetic data from liquid- and solid-phase models. *J. Colloid Interface Sci.*, *292*: 363.
40. Cestari, A.R.; Vieira, E.F.S.; Vieira, G.S.; Almeida, L.E. (2006) The removal of anionic dyes from aqueous solutions in the presence of anionic surfactant using aminopropylsilica. -A kinetic study. *J. Hazard. Mater.*, *138*: 133.
41. Vieira, E.F.S.; Cestari, A.R.; Lopes, E.C.N.; Barreto, L.S.; Lázaro, G.S.; Almeida, L.E. (2007) Determination of kinetic parameters from isothermal calorimetry for interaction processes of pyrimethamine with chitosan derivatives. *React. Funct. Polym.*, *67*: 820.
42. Zubieta, C.E.; Messina, P.V.; Luengo, C.; Dennehy, M.; Pieroni, O.; Schulz, P.C. (2008) Reactive dyes remotion by porous TiO_2-chitosan materials. *J. Hazard. Mater.*, *152*: 765.
43. Royer, B.; Cardoso, N.F.; Lima, E.C.; Vaghetti, J.C.P.; Simon, N.M.; Calvete, T.; Veses, R.C. (2009) Applications of Brazilian-pine fruit shell in natural and carbonized forms as adsorbents to removal of methylene blue from aqueous solutions – Kinetic and equilibrium study. *J. Hazard. Mater.*, *164*: 1213.
44. Lazarin, M.; Airoldi, C. (2004) Intercalation of methylene blue into barium phosphate – synthesis and electrochemical investigation. *Anal. Chim. Acta*, *523*: 89.
45. Aroguz, A.Z.; Gulen, J.; Evers, R.H. (2008) Adsorption of methylene blue from aqueous solution on pyrolyzed petrified sediment. *Bioresour. Technol.*, *99*: 1503.
46. El-Qada, E.N.; Allen, S.J.; Walker, G.M. (2008) Adsorption of basic dyes from aqueous solution onto activated carbons. *Chem. Eng. J.*, *135*: 174.
47. Al-Qodaha, Z.; Lafi, W.K.; Al-Anber, Z.; Al-Shannag, M.; Harahsheh, A. (2007) Adsorption of methylene blue by acid and heat treated diatomaceous silica. *Desalination*, *217*: 212.
48. Al-Futaisi, A.; Jamrah, A.; Al-Hanai, R. (2007) Aspects of cationic dye molecule adsorption to palygorskite. *Desalination*, *214*: 327.
49. Xun, Y.; Shu-Ping, Z.; Wei, X.; Hong-You, C.; Xiao-Dong, D.; Xin-Mei, L.; Zi-Feng, Y. (2007) Aqueous dye adsorption on ordered mesoporous carbons. *J. Colloid Interface Sci.*, *310*: 83.
50. Messina, P.V.; Schulz, P.C. (2006) Adsorption of reactive dyes on titania–silica mesoporous materials. *J. Colloid Interface Sci.*, *299*: 305.
51. Shawabkeh, R.A. (2004) Synthesis and characterization of activated carbo-aluminosilicate material from oil shale. *Microporous Mesoporous Mater.*, *75*: 107.
52. Tsai, W.T.; Hsien, K.J.; Yang, J.M. (2004) Silica adsorbent prepared from spent diatomaceous earth and its application to removal of dye from aqueous solution. *J. Colloid Interface Sci.*, *275*: 428.
53. Hsieh, C.T.; Fan, W.S.; Chen, W.Y. (2008) Impact of mesoporous pore distribution on adsorption of methylene blue onto titania nanotubes in aqueous solution. *Microporous Mesoporous Mater.*, *116*: 677.
54. Li, L.; Wang, S.; Zhu, Z. (2006) Geopolymeric adsorbents from fly ash for dye removal from aqueous solution. *J. Colloid Interface Sci.*, *300*: 52.

Downloaded At: 08:54 25 January 2011